

Computational Studies of Cell Durotaxis on Extracellular Matrix Rigidity Gradients as a Model for Wound Healing and Fibrosis



Chieng Ling Poh

Abstract Durotaxis is the phenomenon where cells migrate towards stiffer regions on a substrate surface, and has important significance in biological processes and diseases such as wound healing or fibrosis, where rigidity gradients of the extracellular matrix may influence cell migration. However, studies on durotaxis are often limited by the difficulty in creating substrates with smooth stiffness gradients or creating very soft substrates and gels for experimentation, hence the need for a computational model. In this study, we developed a computational model for simulation of cell durotaxis, and analysed the behaviour of durotactic efficiency in response to varying stiffness gradients, and the dependence of durotaxis on absolute rigidity of substrates. The model involves a cell consisting of ordered or randomly aligned actin filaments, which exert traction forces on the substrate causing cell migration. It was found that durotactic efficiency increases with increasing substrate stiffness gradient, and there exists a threshold stiffness gradient required in order to induce effective durotaxis. Besides rigidity gradient, absolute rigidity also affects durotaxis. As absolute rigidity increases, efficiency of durotaxis first increases then decreases, with durotaxis being the most efficient on substrate of intermediate stiffness. Increased extracellular matrix rigidity is correlated with increased severity of disease, thus increased durotactic efficiency leads to increased number of cells migrating to the area for healing and repair. A threshold gradient for durotaxis may be necessary to prevent a noisy substrate of fluctuating rigidity from being interpreted as a rigidity gradient, thus gradient needs to be high enough for durotaxis.

Keywords Durotaxis · Rigidity gradient · Computational model

1 Introduction

Cells have long been demonstrated to migrate towards stiffer regions on a substrate surface in a phenomenon known as durotaxis [1, 2]. Such cell migration has important

C. L. Poh (✉)

NUS High School of Mathematics and Science, Singapore, Singapore

e-mail: h1510105@nushigh.edu.sg

© The Author(s), under exclusive license to Springer Nature Singapore Pte Ltd. 2021

H. Guo et al. (eds.), *IRC-SET 2020*,

https://doi.org/10.1007/978-981-15-9472-4_14

163

biological significance, as rigidity of the extracellular matrix (ECM) may influence cell migration in biological processes such as wound healing and diseases such as fibrosis. Increase in rigidity of the ECM during wound healing [3] may influence the migration of cells necessary for wound healing towards the site of the wound, which may in turn influence the healing process and formation of new tissue. Stiffening of tissue and the ECM in fibrosis [4] may also influence migration of cells involved in fibrosis. Although the exact mechanisms involved in cell durotaxis are still unknown, substrate rigidity has been known to influence various aspects of the cell, including actin polymerization [5, 6], focal adhesion stability [2, 5–7], and ability to generate traction forces [2, 5]. Stiffer substrate is known to correlate with increased ordering of actin filaments [5], higher actin polymerization [6, 8], more stable focal adhesions [5–8] and increased traction forces [2, 5]. These responses can be used to construct a computational model for cell durotaxis. The cell can be modelled as a circle containing many rods representing actin filaments. On stiff substrates, actin filaments are increasingly ordered in one direction, while on softer regions, the actin filaments are less ordered and arranged randomly in different orientations. The cell exerts traction forces on the substrate through actomyosin contractions through the actin filaments, and by Newton's third law, the substrate exerts an equal and opposite force on the cell. As the actin filaments are more ordered in a single direction on stiff substrates, the traction forces from each actin filament add up to produce a large net force, while on softer substrate, the force vectors in different directions cancel out to produce a small net force. The greater force experienced by the cell on the stiff region allows the cell to be pulled towards the stiffer region on the substrate. A schematic diagram of the cells and actin filaments can be found in Figs. 2 and 3 in the appendix. Though cells have been known to migrate towards stiffer substrate along rigidity gradients [1, 7, 9], little has been done to analyse the behaviour of durotactic efficiency in response to varying gradients, such as investigating the existence of a threshold gradient or the rate of change of durotactic efficiency in response to changing rigidity gradients. In addition, not many studies have been done to investigate the dependence of durotaxis on the absolute rigidity of substrates, instead of just considering the rigidity gradient. Even so, the scope of these studies are usually limited by the difficulty in creating substrates with completely smooth stiffness gradients [10], or creating very soft substrates and gels for experiments, thus not much analysis is done on very soft substrates. Hence, a computational model is relevant and necessary for us to predict the results of these experiments that are difficult to replicate in real life. In this study, we evaluated a durotactic index (DI) to represent the durotactic efficiency of cells on a substrate, and used our computational model to investigate the behaviour of DI with changing substrate stiffness gradients, and dependence of DI on absolute rigidity of the substrate (Fig. 1).

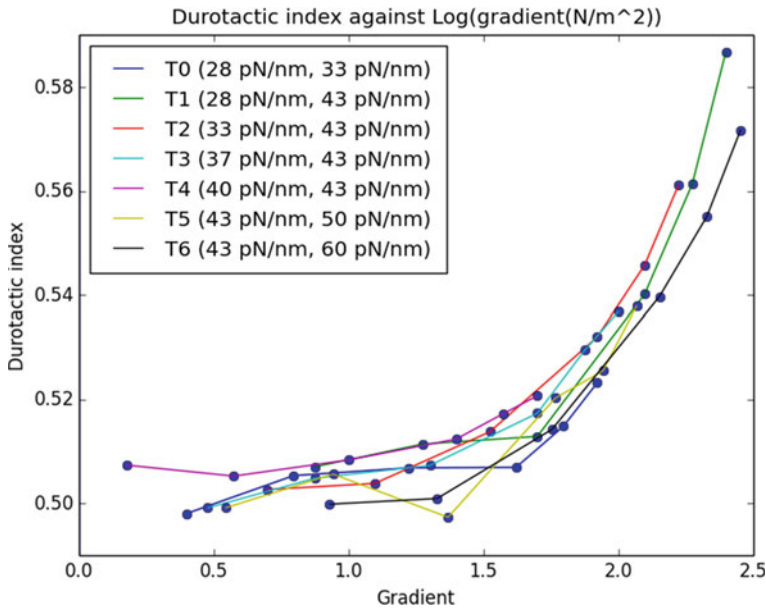


Fig. 1 Summary graph of Durotactic index against rigidity gradient at different absolute rigidities. The softest and stiffest stiffnesses of the gradients for each condition T0–T6 are shown. Each data point is the average DI of 2000 simulated cells

2 Methods

We modelled a cell as a circle of radius $30 \mu\text{m}$ on a substrate consisting of a soft and stiff region located a horizontal distance away from each other, with a uniform stiffness gradient between the two regions. The position of the cell is represented in a coordinate system with $x = 0$ equidistant from both regions. The stiff region is always on the right of the soft region. Let x_1 and x_2 be the x -coordinates of the boundaries of the soft and stiff regions respectively in μm , so that $x_1 = -x_2$ (x_2 is positive and x_1 is negative). Let E_1 and E_2 be the stiffness of the soft and stiff regions respectively in pN/nm , let x be the x -coordinate of a point and let E be the stiffness at that point. When $x < x_1$, $E = E_1$. When $x > x_2$, $E = E_2$. When $x_1 < x < x_2$, stiffness varies linearly with x , so $E = \frac{E_2 - E_1}{x_2 - x_1}x + \frac{E_1 + E_2}{2}$. $\frac{E_2 - E_1}{x_2 - x_1}$ gives the magnitude of the stiffness gradient in kN/m^2 .

A. Generation of rod filaments

Each cell has 35 rods of length $15 \mu\text{m}$ each, representing actin filaments. The centre of each rod is positioned randomly within the cell. The circle formed by the rod when rotated 360° about its centre should be completely within the cell.

B. Generation of rod filament angles

Substrate stiffness E at the rod centre is used to calculate an order parameter S of the rod. Actin filaments are more ordered on stiffer substrate, so S increases as E increases [5]. From experimental data from Fig. 4e of Gupta et al. [5], we approximate a function of S against E that fits the experimental data [5]. Thus we define the order parameter S to be increasing linearly from 0 at 30 pN/nm to 0.65 at 100 pN/nm, with $S = 0$ for E below 30 pN/nm. S at any E above 30 pN/nm can be obtained by $S = \frac{13}{1400}E - \frac{39}{140}$. A graph of S against E can be found in Fig. 4 in the appendix. The angle for each rod is sampled from a von Mises distribution with $\mu = 0$ and $\frac{1}{\kappa} = 9.841e^{-28.79S} + 2.324e^{-4.183S}$. This is the angle between the rod and the positive x -axis. Output angles above 90° or below -90° are adjusted by subtracting the angle from 90° and -90° respectively, so that all angles are adjusted to be within -90° to 90° .

C. Generation of traction forces

E at the rod is now defined as the stiffness at the end of the rod further away from the cell centre, instead of at the rod centre. Using experimental data from Fig. 4g of Gupta et al. [5], we approximate a function of traction force against E that fits the experimental data obtained [5]. From the data, we can define the traction force as

$$\begin{aligned} F_{traction} = & (-2.998 \times 10^{-10})E^6 + (9.941 \times 10^{-8})E^5 \\ & - (1.297 \times 10^{-5})E^4 + 0.0008521E^3 - 0.03028E^2 \\ & + 0.6138E + 0.02629 \end{aligned}$$

where E is in pN/nm and force is in pN. A graph of this function can be found in Fig. 5 in the appendix. This is the traction force associated with that actin filament, exerted by the cell on the substrate. It points from the end of the rod further away from the cell centre to the end of the rod closer to the cell centre. The x - and y - components of the force vectors from all 35 rods are summed to obtain the total force by the cell in the x and y directions.

D. Generation of random forces

A random force adds random motion to the cell. A θ is sampled from a von Mises distribution with $\mu = 0$ and $\kappa = 10^{-5}$. The x - and y -components of the force (in pN) are defined as $F_{xrandom} = 18.648\cos(\theta)$ and $F_{yrandom} = 18.648\sin(\theta)$ respectively.

E. Moving the cell

The total force exerted by the cell consisting of the traction forces and random force are summed to obtain the total force F_{total} in the x and y directions. The force exerted on the cell by the substrate is of equal magnitude but opposite in direction. By manipulation of Eq. (2) of Zeng et al. [11], we obtain an equation describing the displacement of the cell depending on force exerted [11]. Reducing the equation, we define the displacements in the x - and y -directions, Δx and Δy to be $\Delta x =$

$-0.3F_{x_{total}}$, and $\Delta y = -0.3F_{y_{total}}$ respectively. The negative signs reflect the fact that the force exerted on the cell is in the opposite direction to the force the cell exerts.

F. Calculation of durotactic index, DI

The entire process was repeated 72 times for each cell for a total of 72 time steps. If the position of the cell centre at the start of a time step is within the stiffness gradient range ($x_1 \leq x \leq x_2$), that time step is included in calculation of DI. The time step is durotactic if the angle of the displacement vector of the cell relative to the positive x-axis, α , falls within a predetermined range of angles. When $0 < \cos(\alpha) \leq 1$ ($-90^\circ < \alpha < 90^\circ$) as in our model, the time step is durotactic as long as displacement is in the positive x-direction (towards stiffer region). However, a narrower range of values of α can be used if a stricter requirement for durotaxis is desired. The DI of the cell is defined as ratio of number of durotactic time steps divided by total number of time steps (where $x_1 \leq x \leq x_2$). Greater extent of durotaxis corresponds to higher DI. Since $0 < \cos(\alpha) \leq 1$, the expected DI for random motion is 0.5.

G. Dependence of DI on gradient

A substrate of some E1 and E2 was subjected to 6 sets of values of x_1 and x_2 in Figure A2d in the appendix to obtain 6 different rigidity gradients but same rigidity on the soft and stiff regions. x_1 and x_2 were restricted such that $x_2 - x_1 \geq 60 \mu m$, as diameter of the cell is $60 \mu m$ and it would be difficult for the cell to feel the change in stiffness along the gradient if one end of the cell reaches the stiff side before the other leaves the soft side and vice versa. For each gradient, 2000 cells were simulated with half starting at x_1 and half at x_2 . The DI of this gradient is the average DI of all 2000 cells. DI was plotted against $\log(\text{gradient})$. A logarithmic scale is used for gradients as skewness in values makes the results hard to visualize together. The above was repeated for different E1 and E2 in Figure A2c in the appendix. Thus we obtain 7 plots of DI against $\log(\text{gradient})$, each corresponding to a condition T0–T6.

3 Results

A. Durotactic efficiency increases with rigidity gradient

Based on the graph obtained, the DI showed a general increasing trend as gradient increases for all conditions. Analysing the cell trajectories of cells in condition T2 on gradients of 167 N/m^2 (DI 0.56, Fig. 6) and 5 N/m^2 (DI 0.50, Fig. 7), cell trajectories on the 167 N/m^2 gradient show migration towards the stiffer region of the substrate (towards the right) compared to cells on the 5 N/m^2 gradient, which showed roughly equal movement of cells in both directions. This confirms that the extent of durotaxis of cells on the substrate did indeed increase due to the increase in gradient.

B. Existence of threshold gradient required to induce durotaxis

The different values of $E1$ and $E2$ used in the different conditions allow us to compare substrates with same or similar gradients but of different absolute rigidity. From $T0$ to $T6$, the absolute rigidity of the substrate becomes stiffer as the average rigidity of the substrate increases. For all conditions, DI stays relatively constant at about 0.5 (indicating random motion) for a range of gradients before it starts to increase exponentially past a certain gradient value. This suggests the existence of a threshold rigidity gradient required for durotaxis to occur.

C. *Durotaxis is most optimal on intermediate stiffness*

Past the threshold, DI generally increases with gradient, but at different rates for different conditions. Substrates of the same gradient but different absolute rigidity have different DI . Thus other than rigidity gradient, absolute rigidity is also a factor in determining the durotactic efficiency of cells on the substrate. For gradients past the threshold, $T2$ is observed to have the highest DI when compared to other substrates at the same gradient, followed by $T4$, $T3$, $T1$, $T5$, $T6$ then $T0$. Since average rigidity of the substrate increases from $T0$ – $T6$, durotaxis is most efficient on substrate of intermediate stiffness, and cells on substrates that are softer or stiffer than the optimal stiffness range do not exhibit efficient durotaxis. Generally, the observed trend is that as substrate stiffness increases, durotactic efficiency first increases until an optimal stiffness then decreases as the substrate becomes stiffer. A substrate with higher durotactic efficiency would also be expected to have lower threshold gradient, which is identified by the point where DI starts to increase exponentially after staying constant at about 0.5. From the graph, $T2$ has the lowest threshold gradient of 12.5 N/m^2 where DI starts increasing, which confirms that $T2$ has the greatest extent of durotaxis out of all the conditions and that durotaxis is indeed most efficient on substrate of intermediate stiffness. The threshold gradients for the other conditions do not strictly follow the general trend that durotactic efficiency increases then decreases as stiffness increases, but these anomalies may be attributed to random variation.

4 Discussion

Since a greater rigidity difference correlates with increased extent of durotaxis, it is expected that DI increases as gradient increases [1]. For substrates with the same rigidity gradient but different absolute rigidity, we found that as absolute rigidity increases, the general trend is that durotactic efficiency first increases then decreases, with most efficient durotaxis occurring on substrate of intermediate stiffness. To understand this phenomenon, we can look at the functions of the order parameter, S (Fig. 4) which determines how aligned the direction of the traction forces are, and magnitude of traction force, F_{traction} (Fig. 5) against substrate stiffness. On a gradient, the two ends of the cell experience different substrate stiffness, so the different forces experienced in two ends of the cell determines the net force on the cell and thus the direction of cell migration. Since the graph of traction force is concave downwards, as rigidity increases, the difference in the magnitude of traction force decreases for

the same difference in substrate stiffness. Thus the net force on the cell decreases and the DI decreases as absolute rigidity of the substrate increases for the same rigidity gradient. At low substrate stiffness, S stays constant at 0 before it starts increasing linearly at $E = 30$ pN/nm. Thus for substrate at low rigidities below 30 pN/nm, the reduced difference in the order parameter values leads to decreased extent of durotaxis. Thus for substrates of the same rigidity gradient, durotaxis is most efficient on substrate of intermediate absolute stiffness and efficiency is reduced if the substrate is too soft or too stiff. As substrate rigidity increases, DI first increases until an optimum stiffness, then decreases as the substrate becomes stiffer. The latter trend was also observed by DuChez et al. [9] and Moriyama and Kidoaki [7], when durotaxis was observed to become more efficient as the substrate becomes softer [7, 9]. Due to the different cell types used, the range of substrate stiffness used in observing this trend in their experiments may not overlap with the range used in our simulation, however the trend of durotactic efficiency increasing with decreasing substrate stiffness was still observed. However, the trend observed in our simulation that durotactic efficiency decreases when substrate rigidity further decreases beyond an optimum stiffness was not observed in both of the above mentioned experiments done by DuChez et al. [9] and Moriyama and Kidoaki [7]. This may be due to the difficulty in making soft substrates and gels compared to hard substrates, thus experimentation was not done on soft substrates that are softer than the stiffness ranges used in these experiments, so durotactic efficiency was not observed to decrease when substrate becomes even softer. If further experimentation was done on even softer substrates softer than those used in these experiments, this additional trend may also be observed. However, due to the difficulty in creating these very soft substrates soft enough to observe this trend, we can only use the results from our computational model to predict the results of these real-life experiments.

Our results can also be explained by considering their biological implications in diseases such as fibrosis or wound healing. Increased stiffness gradient of the extracellular matrix is likely to be correlated with increased severity of disease, such as more scarring or having more stiff fibrotic tissue. Hence, more cells are needed to migrate to the area for increased formation of new healthy tissue for healing and repair, so durotactic efficiency increases on higher rigidity gradients. The existence of a threshold gradient to induce durotaxis ensures that a noisy substrate with randomly fluctuating rigidity will not be misinterpreted as a substrate with a low rigidity gradient, thus gradient needs to be of a high enough value in order to induce durotaxis.

5 Conclusion

In conclusion, we have confirmed the existence of a threshold rigidity gradient that is required in order to induce effective durotaxis. Cells undergo random motion at low rigidity gradients, and past a certain threshold gradient, durotactic efficiency starts to increase with gradient. Absolute rigidity of the substrate also affects the

extent of durotaxis of cells. As absolute rigidity increases, efficiency of durotaxis first increases then decreases, with durotaxis being the most efficient on substrate of intermediate stiffness. Increase of durotactic efficiency with gradient can be correlated with increased number of migratory cells needed for repair due to increased severity of disease, while a threshold gradient for durotaxis may be necessary to prevent a noisy substrate from being interpreted as a rigidity gradient, thus gradient needs to be high enough.

Acknowledgements Thanks to Dr Chiam Keng-Hwee and Dr Yip Ai Kia from Bioinformatics Institute, A*STAR for the constant guidance and support.

Appendix

See Figs. 2, 3, 4, 5, 6 and 7, Tables 1 and 2.

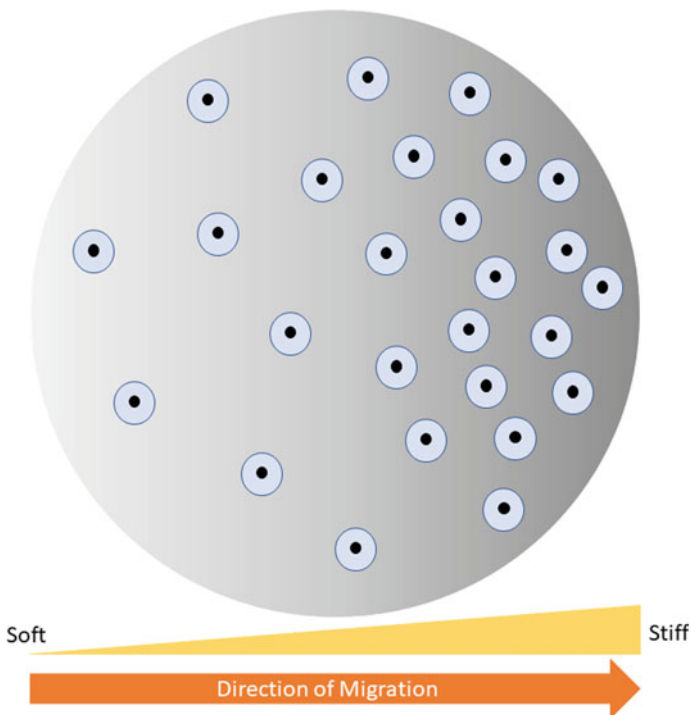


Fig. 2 Schematic diagram of durotactic cell migration of cells towards stiffer substrate on a substrate rigidity gradient

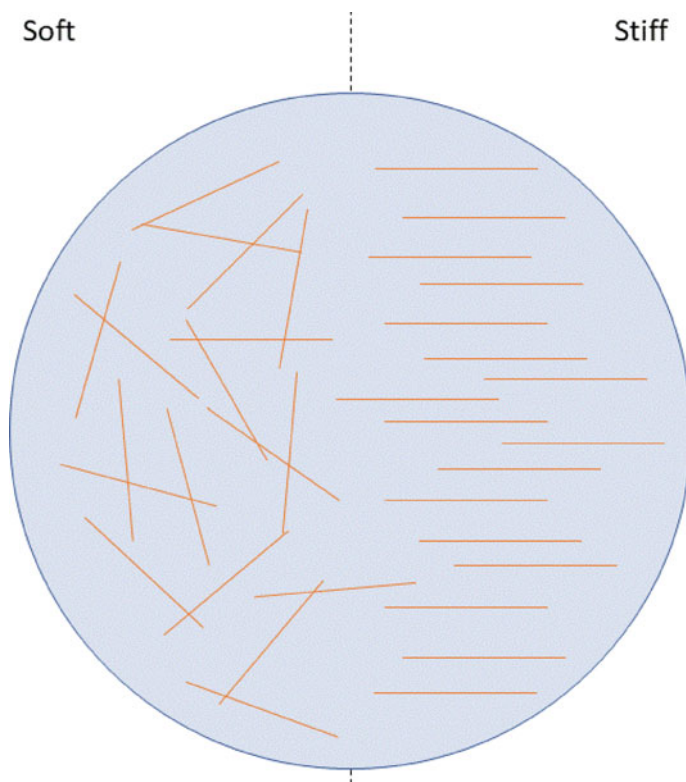


Fig. 3 Schematic of cell and actin filaments. Actin filaments are more ordered on stiff substrate, leading to greater net force on stiffer substrate causing cell migration

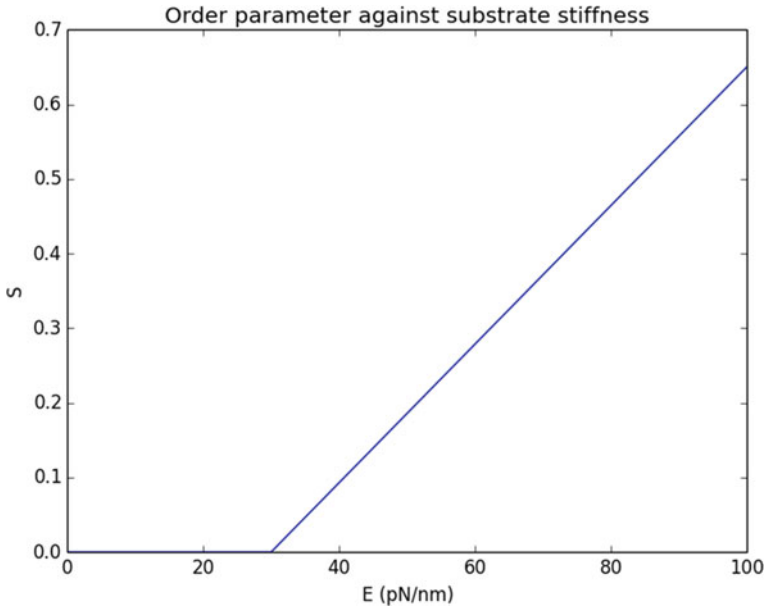


Fig. 4 Graph of order parameter of cell actin filaments against substrate stiffness at cell centre

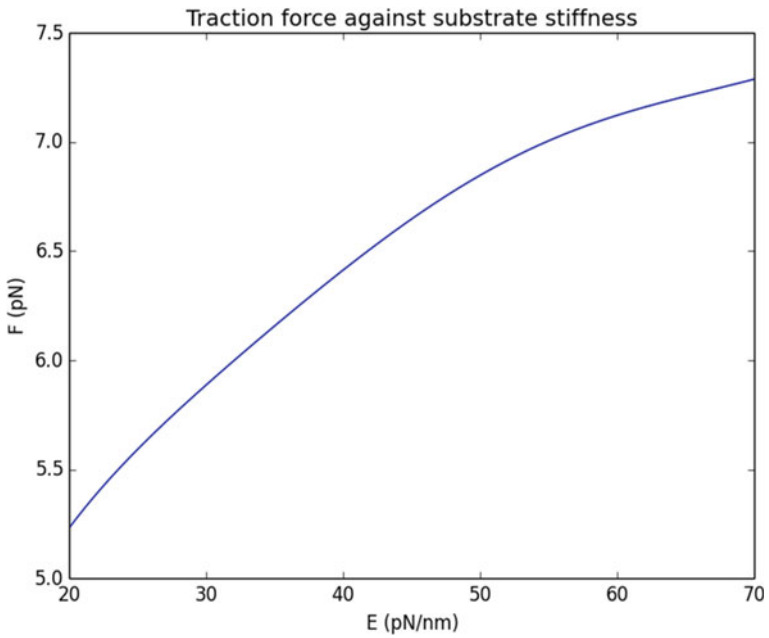


Fig. 5 Graph of traction force exerted by each actin filament against substrate stiffness at actin filament

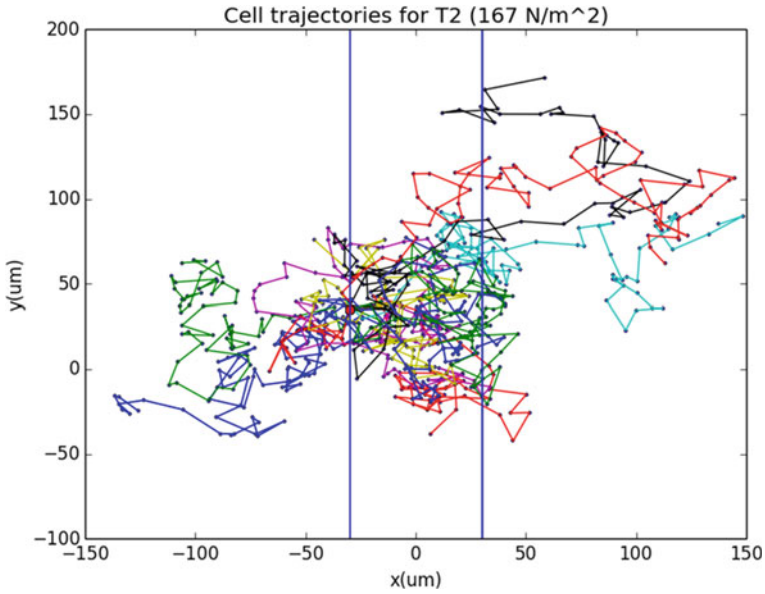


Fig. 6 10 cell trajectories for cells on T2 (between 33 pN/nm and 43 pN/nm) at gradient of 167 N/m² starting at x1 (-30 μm). The red circle represents the starting position of all the cells. Durotactic migration towards stiffer region (right side) can be seen

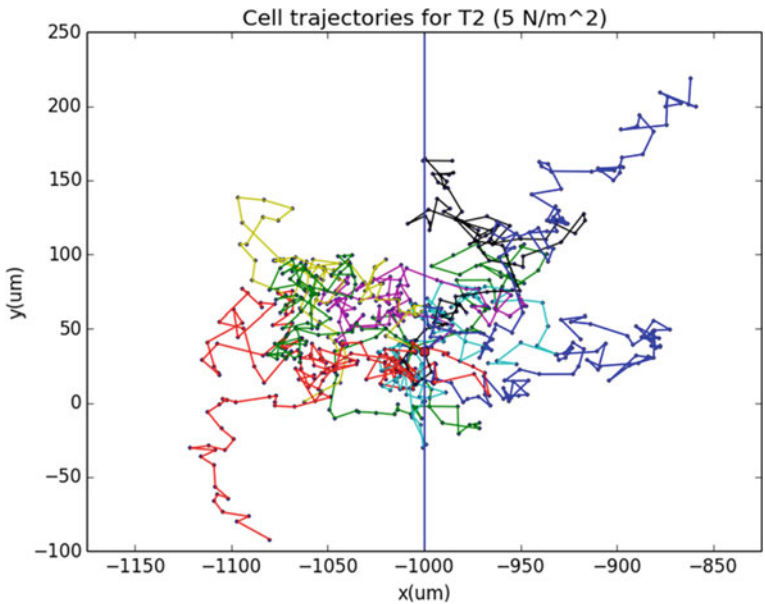


Fig. 7 10 cell trajectories for cells on T2 (between 33 pN/nm and 43 pN/nm) at gradient of 5 N/m² starting at x1 (-1000 μm). The red circle represents the starting position of all the cells. Equal migration of cells in both directions towards both soft and stiff regions, so no durotaxis observed

Table 1 E1 and E2 (softest and stiffest rigidities) used for the rigidity gradients at each condition

Condition	E1 (pN/nm)	E2 (pN/nm)
T0	28	33
T1	28	43
T2	33	43
T3	37	43
T4	40	43
T5	43	50
T6	43	60

Table 2 Values of x1 and x2 used (x-coordinates of boundaries of the substrate stiffness gradient region)

x1 (μm)	x2 (μm)
-30	30
-40	40
-60	60
-150	150
-400	400
-1000	1000

References

- Hassan, A. R., Biel, T., & Kim, T. (2018). Mechanical Interactions between a Cell and an Extracellular Environment Facilitate Durotactic Cell Migration. *bioRxiv*, 460170.
- Lo, C. M., Wang, H. B., Dembo, M., & Wang, Y. L. (2000). Cell movement is guided by the rigidity of the substrate. *Biophysical journal*, 79(1), 144–152.
- Rosińczuk, J., Taradaj, J., Dymarek, R., & Sopol, M. (2016). Mechanoregulation of wound healing and skin homeostasis. *BioMed Research International*, 2016, 1–13.
- Herrera, J., Henke, C. A., & Bitterman, P. B. (2018). Extracellular matrix as a driver of progressive fibrosis. *The Journal of clinical investigation*, 128(1), 45–53.
- Gupta, M., Sarangi, B. R., Deschamps, J., Nematbakhsh, Y., Callan-Jones, A., Margadant, F., ... & Ladoux, B. (2015). Adaptive rheology and ordering of cell cytoskeleton govern matrix rigidity sensing. *Nature communications*, 6, 7525.
- Geiger, B., Spatz, J. P., & Bershadsky, A. D. (2009). Environmental sensing through focal adhesions. *Nature reviews Molecular cell biology*, 10(1), 21–33.
- Moriyama, K., & Kidoaki, S. (2018). Cellular durotaxis revisited: Initial-position-dependent determination of the threshold stiffness gradient to induce durotaxis. *Langmuir*, 35(23), 7478–7486.
- Hirata, H., Tatsumi, H., & Sokabe, M. (2008). Mechanical forces facilitate actin polymerization at focal adhesions in a zyxin-dependent manner. *Journal of cell science*, 121(17), 2795–2804.
- DuChes, B. J., Doyle, A. D., Dimitriadis, E. K., & Yamada, K. M. (2019). Durotaxis by human cancer cells. *Biophysical journal*, 116(4), 670–683.
- Sunyer, R., Jin, A. J., Nossal, R., & Sackett, D. L. (2012). Fabrication of hydrogels with steep stiffness gradients for studying cell mechanical response. *PloS one*, 7(10), e46107.
- Zeng, Y., Yip, A. K., Teo, S. K., & Chiam, K. H. (2012). A three-dimensional random network model of the cytoskeleton and its role in mechanotransduction and nucleus deformation. *Biomechanics and modeling in mechanobiology*, 11(1–2), 49–59.